Transverse coincidence structures in spontaneous parametric down-conversion with orbital angular momentum: Theory

Geraldo A. Barbosa*

Department of Electrical Engineering and Computer Science, Center for Photonic Communication and Computing, Northwestern University, 2145 North Sheridan Road, Evanston, Illinois 60208-3118, USA

(Received 10 April 2007; published 19 September 2007)

Coincidence structures in the transverse plane of type-II spontaneous parametric down-conversion carrying orbital angular momentum are obtained. Azimuthal symmetry breaking around the pump beam direction reveals itself on these quantum images. Analytical expressions for the amplitude probability of the down-conversion process are shown including the nonlinear polarizability components.

DOI: 10.1103/PhysRevA.76.033821 PACS number(s): 42.65.Lm, 42.50.Ct, 42.60.Jf, 42.65.−k

I. INTRODUCTION

Entanglement of photon states carrying orbital angular momentum (OAM) is a tool in quantum optics. These states have been experimentally produced by spontaneous parametric down-conversion (SPDC) [1]. They were predicted [2] subjected to certain symmetry conditions that are still subject to some controversy. This work will review those arguments in detail and will emphasize the importance of azimuthal symmetry in the SPDC for a complete transfer of OAM from the pump photons to the SPDC photons. Azimuthal symmetry breaking will reflect in a poor transfer of OAM. Among possible cases of asymmetries is the one produced by walk off in type-II SPDC.

Experimentally, these OAM states can be created under the condition of *a posteriori* or *a priori* OAM imprinting by appropriated masks or filter converters. For the *a posteriori* imprinting, the pump beam does not need to carry OAM, but an appropriate OAM mode converter l is inserted onto one of the down converted beams. The conjugate beam is expected to acquire an OAM of $-l$. For the *a priori* imprinting, the pump beam mode is set in an OAM state, say, l. However, as discussed in Ref. [2], the initial OAM l may or may not be transferred to the SPDC. Discussions about if this transfer of OAM occurs or not and if special conditions are needed to have OAM transfer has populated the recent literature sometimes with conflicting answers: "yes," "no," "under certain conditions" (see some references in Ref. [3]). Sometimes, conclusions derived from particular cases, say, under conditions adequate for low wave vectors or paraxial cases (e.g., Ref. [4]), can be mistakenly taken as being general. Part of this nonuniform understanding on this subject derives from oversimplified Hamiltonian or wave states considered (simplified "backbone" models). The difficulties to derive general conclusions taking into account realistic phase matching and light-matter coupling through the nonlinear polarizability tensor sometimes makes these time consuming tasks not appealing. Therefore, it is common that a single proportionality constant replaces an involved angular dependence resulting in a nonrealistic description. Instead of being just technical details, these more complex dependences may be crucial to a full understanding of these processes including entanglement between conjugate photon pairs. Phase matching is also frequently assumed under simplified conditions not sufficient to treat in detail pump modes with amplitudes more complex than a simple Gaussian intensity profile.

Although not claiming a complete analysis of this problem, this paper does not take for granted many of these commonly oversimplified assumptions. It tries to discuss the problem of transfer of OAM between the pump beam and the SPDC photons with reasonable detail. Phase matching conditions dependent on $\chi^{(1)}$ are not oversimplified; also detailed is the dependence of SPDC on $\chi^{(2)}$. This should provide the reader with enough material to help his own work or, at least, to show fundamental elements necessary in this trade. It may also stimulate others to improve our understanding in this area. Certainly, many future applications will demand a careful understanding of the entanglement carried by these nonlinear processes beyond current treatments. Even some small immediate rewards can be obtained such as a method to obtain the nonlinear coefficients in $\chi^{(2)}$ by comparison of experiment and theory.

This paper was written trying to give a newcomer to this field a straightforward view of the involved elements starting from the wave state amplitude describing SPDC. It describes all components involved in this amplitude and details aspects of phase matching including the simplified description of phase matching in two steps: longitudinal and transverse conditions. The nonlinear tensor $\chi^{(2)}$ and the resulting nonlinear polarizability of the medium are discussed, including their transformations between the crystal reference system and the laboratory reference system. This way the reader can dedicated himself to the main aspects presented instead of having to work out technical details. Certainly, for some, most of the presented aspects may be trivial and can be skipped without problems. However, any disagreement between views may result in an overall enlightenment for all.

II. WAVE STATE

The Hamiltonian describing SPDC can be easily found in the literature (e.g., Ref. [5]). It describes free propagating photons from a pump and from the down-conversion process that occurs due to the nonlinear light-matter interaction occurring in an ideally transparent medium (e.g., crystalline

*g-barbosa@northwestern.edu

medium within the crystal band gap). A pump photon will excite the nonlinear medium through a very fast interaction with virtual electrons and decay *either* into a similar pump photon or into two conjugate photons—historically called signal and idler. These virtual interactions as well as the propagation of the SPDC photons occur in the nonisotropic medium with specific symmetries defined by the crystal class involved. Therefore, medium symmetries are built explicitly in $\chi^{(2)}$ and implicitly in $\chi^{(1)}$, defining the nonlinear interaction and the light propagation in the medium. The Hamiltonian for these processes usually neglect coupling to the lattice possibly intermediated by electrons. Although the fast interaction times indicate that this coupling to the lattice should be negligible, this possibility should not be ruled out in general.

At this point, one could remind the reader the uncertainty relationship connecting angular momentum and phase uncertainties [6]

$$\Delta L_z \Delta \phi \geq \frac{\hbar}{2}|1 - 2\pi P(\phi_0)|. \tag{1}$$

It states that a large uncertainty in angle allows L_z to have a small uncertainty. Consequently, in order to guarantee precision in L_z, uncertainty in ϕ has to be maximum [7]. Could the medium symmetries (built in $\chi^{(2)}$ and $\chi^{(1)}$) cause restrictions on the photon interactions or propagation that could somewhat constrain the associated azimuthal angle ϕ and therefore do not allow its maximum uncertainty to be achieved? This problem has been discussed in Ref. [2] but it will be detailed here for clarity.

The interaction Hamiltonian H_I gives the wave state $|\psi(t)\rangle = \exp[(-i/\hbar)\int_{t-\tau}^{t} H_I(\tau')d\tau']|0\rangle$, from which successful spontaneous photon conversion in first order is

$$|\psi(t)\rangle = \sum_{s,s'} \int d^3k' \int d^3k F_{s,s'}(\mathbf{k},\mathbf{k}')\hat{a}^\dagger(\mathbf{k},s)\hat{a}^\dagger(\mathbf{k}',s')|0\rangle. \tag{2}$$

The probability amplitude for signal and idler at $(\mathbf{k},\mathbf{k}')$ is $F_{s,s'}(\mathbf{k},\mathbf{k}') = A_{\mathbf{k},s;\mathbf{k}',s'} l_E^{(*)}(\omega_\mathbf{k}) l_E^{(*)}(\omega_{\mathbf{k}'}) T(\Delta\omega)\tilde{\psi}_{lp}(\Delta\mathbf{k})$. $A_{\mathbf{k},s;\mathbf{k}',s'} = \chi^{(2)}_{1jk}[(\mathbf{e}_{\mathbf{k},s})^*_j(\mathbf{e}_{\mathbf{k}',s'})^*_k + (\mathbf{e}_{\mathbf{k}',s'})^*_j(\mathbf{e}_{\mathbf{k},s})^*_k]$, $(\mathbf{e}_\mathbf{k},\mathbf{e}_{\mathbf{k}'})$ are unitary polarization vectors for signal and idler photons, $l_E^{(*)}(\omega) = -i\sqrt{\hbar\omega/2\epsilon(\mathbf{k},s)}$, $\tilde{\psi}_{lp}(\Delta\mathbf{k}) = \int_{V_I} d^3r \psi_{lp}(\mathbf{r})\exp(-i\Delta\mathbf{k}\cdot\mathbf{r})$ and ψ_{lp} is the Laguerre-Gaussian pump field amplitude in $\mathbf{E}(r,\phi,z;t) = \psi_{lp}(\mathbf{r})e^{i(k_P z - \omega_P t)}\hat{\mathbf{e}}_1$. $T(\Delta\omega) = \exp[i\Delta\omega(t - \tau/2)]\sin(\Delta\omega\tau/2)/(\Delta\omega/2)$ is the time window function defining the $\Delta\omega$ range given the interaction time τ, $\Delta\omega = \omega_\mathbf{k} + \omega_{\mathbf{k}'} - \omega_P$, $\Delta\mathbf{k} = \mathbf{k} + \mathbf{k}' - \mathbf{k}_P$. Symmetries associated with the crystalline medium influence $A_{\mathbf{k},s;\mathbf{k}',s'} \times \tilde{\psi}_{lp}(\Delta\mathbf{k})$ through $\chi^{(2)}$, $\chi^{(1)}$ and the polarization vectors [2].

It was derived in Ref. [2] that in order for a wave state of a one-photon field $|\psi(t)\rangle_1$ to be an eigenfunction of J_z (or L_z for processes where $S_z = 0$, as will be assumed here) it has to obey $J_z|\psi(t)\rangle_1 = l\hbar|\psi(t)\rangle_1$. This directly gave

$$|\psi(t)\rangle_1 = \sum_s \int d^3k g(k_\rho, k_z, s; t) e^{il\phi} a^\dagger(\mathbf{k},s)|0\rangle. \tag{3}$$

In this condition one can see that the azimuthal phase should occur only as a phase term in the wave state and not in its amplitude. This guarantees that the magnitude square of the integrand presents complete rotational symmetry in ϕ or, equivalently, presents a complete uncertainty in ϕ, as required by Eq. (1). In SPDC, this condition has to be applied both to signal and idler photons. This implies that for perfect OAM transfer from pump photons to SPDC photons, the probability amplitude $F_{s,s'}(\mathbf{k},\mathbf{k}')$ in Eq. (2) should contain the azimuthal angles for signal and idler only as phase terms $e^{im\phi}$ and $e^{in\phi'}$. As a linear superposition of wave functions is also a wave function, superpositions of expressions similar to Eq. (2) containing similar phase terms can also represent a valid solution. However, the superposition coefficients should not depend on the azimuthal angles.

Starting from the accepted standard wave state for SPDC, one may expand the most relevant terms to compare with symmetry restrictions imposed by Eq. (3) and verify if a specific SPDC process may or may not transfer OAM to the down converted photons or even if this transfer can be partial. This answer should not be ambiguous and the result obtained should be general enough to allow direct comparison with specific experiments.

III. THE WAVE STATE AMPLITUDE $F(\mathbf{k}_s,\mathbf{k}_i)$

The wave state amplitude $F(\mathbf{k}_s,\mathbf{k}_i)$ [see Eq. (2)] is the term that needs to be considered in detail. In principle, this amplitude contains a wealth of information one could obtain from the wave state, from efficiency considerations to phase matching conditions. Of course, one has to assume complementary information about the crystalline medium including the light propagation conditions given by the Fresnel equations. From the wave state amplitude the required conditions for phase matching emerge naturally.

The term $A_{\mathbf{k},s;\mathbf{k}',s'}$ will be considered in a separate section and the time window term $T(\Delta\omega)$ admits easy interpretations. For example, for a continuous wave (CW) laser where the interaction time τ can be made large $T(\Delta\omega) \to \pi\delta(\Delta\omega)$. The most involved term is the Fourier transform $\tilde{\psi}_{lp}(\Delta\mathbf{k})$. A careful consideration of this term allows one to derive main conclusions about the SPDC process in general.

A. The Fourier transform $\tilde{\psi}_{lp}(\Delta\mathbf{k})$

The Fourier transform $\tilde{\psi}_{lp}(\Delta\mathbf{k})$ of $\psi_{lp}(\Delta\mathbf{k})$ can be written

$$\tilde{\psi}_{lp}(\Delta\mathbf{k}) = \int_{z_0 - l_c/2}^{z_0 + l_c/2} dz \int_0^{2\pi} d\phi \int_0^\infty dr \psi_{lp}(r,\phi,z) \times e^{-i(\Delta k_x r\cos\phi + \Delta k_y r \sin\phi + \Delta k_z z)}, \tag{4}$$

where

$$\psi_{lp}(r,\phi,z)=\frac{A_{lp}}{\sqrt{1+(z/z_R)^2}}\left[\frac{r\sqrt{2}}{w(z)}\right]^l L_p^l\left[\frac{2r^2}{w(z)^2}\right]\times\exp\left[-i\left(\frac{k_P r^2 z}{2q(z)}+l\tan^{-1}\frac{y}{x}\right)\right]\times\exp\left[i(2p+l+1)\tan^{-1}\frac{z}{z_R}\right],\tag{5}$$

and $w^2=w_0^2[1+(z^2/z_R^2)], q(z)=z+iz_R, w_0^2=(2z_R/k_P), z_0$ gives the crystal center, $r^2=x^2+y^2$, and l_c is the crystal length along the propagation direction. Development of integral (4) in r and ϕ is straightforward although cumbersome:

$$\tilde{\psi}_{lp}(\Delta\mathbf{k})=\pi A_{lp}\left(\frac{i}{2}\right)^l\left(\frac{z_R}{k_P}\right)^{1+l/2}e^{-il\pi/2}\rho_k^l L_p^l\left(\frac{z_R}{k_P}\rho_k^2\right)\times e^{-z_R\rho_k^2/(2k_P)}e^{il\tan^{-1}(\Delta k_y/\Delta k_x)}\times\int_{z_0-l_c/2}^{z_0+l_c/2}e^{i(-1+l+2p)\tan^{-1}(z_R/z)}e^{i(1+l+2p)\tan^{-1}[z/(2z_R)]}\times e^{-i\Delta k_z z}dz,\tag{6}$$

where $\rho_k^2=\Delta k_x^2+\Delta k_y^2=\rho^2+\rho'^2+2\rho\rho'\cos(\phi-\phi')$, $\rho=k\sin\theta$ and $\rho'=k'\sin\theta'$.

The remaining z integral can be solved under conditions favorable to experiments. Conditions $z_0=0$ and $l_c\ll z_R$ are most usual. This gives $\tan^{-1}[z/(2z_R)]\to 0$ and $\tan^{-1}(z_R/z)\to\pi/2$; therefore,

$$\tilde{\psi}_{lp}(\Delta\mathbf{k})=-\pi i^{l+1}2^{-l}A_{lp}\left(l_c\frac{z_R}{k_P}\right)e^{i[\pi p+l\tan^{-1}(\Delta k_y/\Delta k_x)]}\times e^{-\xi/2}\xi^{l/2}L_p^l(\xi)\frac{\sin\left[\frac{l_c}{4z_R}(4-2z_R\Delta k_z+\xi)\right]}{\left[\frac{l_c}{4z_R}(4-2z_R\Delta k_z+\xi)\right]},\tag{7}$$

where $\xi\equiv(z_R/k_P)\rho_k^2$. It is interesting to observe the presence of the phase $\tan^{-1}(\Delta k_y/\Delta k_x)$ in $\tilde{\psi}_{lp}(\Delta\mathbf{k})$. It gives several possibilities for entanglement of signal and idler phases ϕ and ϕ' and is a signature of the complexity connecting signal and idler photons on the plane transverse to the propagation direction. The probability for unconstrained signal and idler occurrences $|F_{s,s'}(\mathbf{k},\mathbf{k}')|^2$ will be proportional to

$$|\tilde{\psi}_{lp}(\Delta\mathbf{k})|^2=\pi^2 4^{-l}|A_{lp}|^2\left(l_c\frac{z_R}{k_P}\right)^2 e^{-\xi}\xi^l L_p^l(\xi)^2\times\left(\frac{\sin\left[\frac{l_c}{4z_R}(4-2z_R\Delta k_z+\xi)\right]}{\left[\frac{l_c}{4z_R}(4-2z_R\Delta k_z+\xi)\right]}\right)^2.\tag{8}$$

Equations (7) and (8) are fundamental for SPDC. Together with $A_{\mathbf{k},s;\mathbf{k}',s'}$ they determine probabilities of signal and idler occurrences and, by state superpositions with arbitrary phases, interferences. Phase matching are determined by the loci of maxima of these same equations.

IV. PHASE MATCHING

Phase matching conditions with variables Δk_z and ξ can be obtained from $|\tilde{\psi}_{lp}(\Delta\mathbf{k})|^2$. In principle, polar and azimuthal angles that define maxima of $|\tilde{\psi}_{lp}(\Delta\mathbf{k})|^2$ should be determined simultaneously, but simplified solutions are frequently used according to the level of detail one requires. For example, since $\sin x/x$ in Eq. (8) is weakly dependent on ξ, Eq. (8) can be treated as two independent parts for phase matching considerations. One part, in form of $\sin x/x$ gives the Δk_z range and the second or remaining part of the equation sets the width associated with the variable ξ. Write $|\tilde{\psi}_{lp}(\Delta\mathbf{k})|^2=f_{\text{long}}\times f_{\text{transv}}$, where $f_{\text{long}}=(\sin x/x)^2$ and $f_{\text{transv}}=\pi^2 4^{-l}|A_{lp}|^2(l_c z_R/k_P)^2 e^{-\xi}\xi^l L_p^l(\xi)^2$. f_{long} can be considered non-negligible from $\Delta k_{z\min}=(4+\xi)/2z_R\simeq 2/z_R$ to $\Delta k_{z\max}=[l_c(4+\xi)-4\pi z_R]/2l_c z_R$ (for $x=\pi$). For $l_c\ll 1$, $\Delta k_z=\pm 2\pi/l_c$. This sets the polar angles θ_{pm} and θ'_{pm} for phase matching. Maxima for f_{transv} will describe azimuthal angles, ϕ and ϕ', and θ_{pm} and θ'_{pm}, that are the polar angle values defined from $\Delta k_{z\min}$ to $\Delta k_{z\max}$. These maxima are not hard to find for specific values of l and p.

Just to exemplify a simplified use of Eq. (8), one can calculate the probability for signal and idler occurrences in a specific Type II case of a uniaxial crystal where the pump beam carries an $l=4$ OAM. The calculations are done for a beta-barium borate (BBO) crystal with the crystal axis inclined by θ_c with respect to the pump beam propagation direction. Two natural coordinate systems are involved, the crystal and the laboratory axes. While descriptions of the linear and nonlinear susceptibilities are usually given in the crystal reference system, the pump beam and the characteristic SPDC pattern desired define the laboratory system to be used. Appropriate coordinate transformations have to be applied to provide correct answers. Starting with the longitudinal equation for phase matching, some additional information needed for its solution will be presented. This additional information will also be used for the transverse phase matching conditions.

A. Longitudinal condition

Expanding Δk_z in the longitudinal condition gives the interval where an appreciable contribution is found, $\Delta k_z=\pm 2\pi/l_c$. That is to say, for angles bounded by this condition, there is a good probability to find signal and idler photons. Let us rewrite this condition in a more tight bound and expand Δk_z,

$$-k_P+(k\cos\theta+k'\cos\theta')\simeq\frac{2\pi}{l_c}.\tag{9}$$

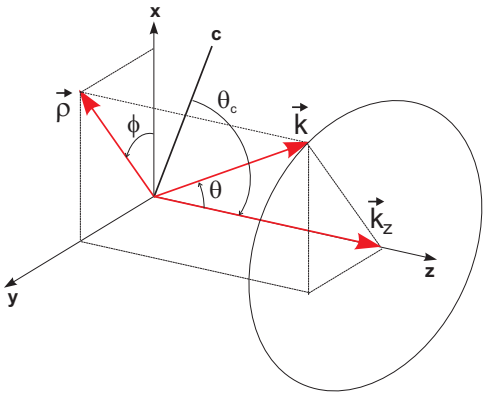

FIG. 1. (Color online) Decomposition of a wave vector **k** into transversal (ρ) and longitudinal ($\mathbf{k}_z$) components in the laboratory axis (x,y,z). A rotation around the y axis by θ_c separates the crystal principal axis from the pump beam propagation direction z.

The wave vectors in the medium are $k=(2\pi/\lambda)n=(\omega/c)n$ and $k'=(2\pi/\lambda')n'=(\omega'/c)n'$, where λ and λ' are vacuum wavelengths and the refractive indexes n and n' have to be found using Fresnel's equations for specific propagation directions and Sellmeier's equations for the principal refractive indexes.

1. Fresnel's equations

Fresnel's equations can provide the refractive index n of a uniaxial crystal along an arbitrary propagation direction specified by the wave vector $\mathbf{k}=(\omega n/c)\hat{\mathbf{s}}$ where the unit vector is $\hat{\mathbf{s}}=s_x\hat{\mathbf{x}}+s_y\hat{\mathbf{y}}+s_z\hat{\mathbf{z}}$. They are derived [10] starting from Maxwell's equations written in local variables, $\hat{\mathbf{s}}\cdot\mathbf{H}=0$, $\mathbf{D}\cdot\hat{\mathbf{s}}=0$, $\mathbf{H}\times\hat{\mathbf{s}}=\mathbf{D}/n$, $\mathbf{E}\times\hat{\mathbf{s}}=-\mathbf{H}/n$, where ∇ was written as $\nabla\rightarrow i(\omega n/c)\hat{\mathbf{s}}$. Eliminating $\mathbf{H}$ results in $\mathbf{D}_j=n^2[\mathbf{E}_j-\hat{\mathbf{s}}_j(\hat{\mathbf{s}}\cdot\mathbf{E})]$. Considering a uniaxial crystal ($\epsilon_{ij}=\epsilon_{ii}\delta_{ij}$) and multiplying both members by s_j one obtains $\epsilon_{jj}E_j-n^2E_j=-n^2[s_j(\hat{\mathbf{s}}\cdot\mathbf{E})]$, which gives $1=-n^2s_j^2/(\epsilon_{jj}-n^2)$. Subtracting 1 ($=s_j^2$) from both sides and writing $n^2=\epsilon$, Fresnels's equations are obtained,

$$\frac{s_x^2}{\frac{1}{\epsilon}-\frac{1}{\epsilon_x}}+\frac{s_y^2}{\frac{1}{\epsilon}-\frac{1}{\epsilon_y}}+\frac{s_z^2}{\frac{1}{\epsilon}-\frac{1}{\epsilon_z}}=0, \tag{10}$$

where $s_x=\sin\theta\cos\phi$, $s_y=\sin\theta\sin\phi$, $s_z=\cos\theta$ and $\epsilon_x=\epsilon_y=\epsilon_o$ are the ordinary dielectric constants along the principal axis and $\epsilon_z=\epsilon_e$ is the extraordinary dielectric constant, Eq. (10). Using the notation $r_x=\epsilon/\epsilon_o=r_y$ and $r_z=\epsilon/\epsilon_e$ and multiplying both members of Eq. (10) by $(1-r_x)^2(1-r_z)^2$, one obtains

$$(1-r_x)^2(1-r_z)^2\left[\frac{(1-r_z)(s_x^2+s_y^2)+(1-r_x)s_z^2}{(1-r_x)(1-r_z)}\right]=0. \tag{11}$$

This equation defines that *either* $(1-r_x)(1-r_z)=0$, that gives either $\epsilon=\epsilon_o$ or $\epsilon=\epsilon_e$ (pure ordinary and extraordinary cases), *or* $[(1-r_z)(s_x^2+s_y^2)+(1-r_x)s_z^2]=0$. This last equation can be written as

$$\frac{1}{\epsilon}=\frac{s_x^2+s_y^2}{\epsilon_e}+\frac{s_z^2}{\epsilon_o}. \tag{12}$$

These are the possibilities for light propagation in uniaxial crystals. Either pure ordinary or extraordinary propagation or a mixture of ordinary and extraordinary light propagation. However, these equations define the refraction indexes in the crystal coordinate system. Obtaining the refractive indexes on the laboratory coordinate system demands that rotations are introduced corresponding to the geometrical situation adopted.

2. Rotation matrices

One should be aware that rotation angles do not obey a universal notation and sometimes references for crystal rotation angles may vary even from crystal to crystal in the literature. In particular, complementary angles may be referred to in a similar way. Figure 1 shows a convenient laboratory coordinate system (x,y,z) obtained from the crystal axis by rotation of angle θ_c around the y axis. Usual crystal rotations to utilize better geometries to increase the efficiency of the down-conversion process consist of rotations about, say, one of the crystal secondary axis followed by a rotation on its principal axis. These matrix rotations can be written

$$R_{zy}=R_z(\phi_c)R_y(\theta_c)=\begin{pmatrix}\cos\phi_c & \sin\phi_c & 0\\ -\sin\phi_c & \cos\phi_c & 0\\ 0 & 0 & 1\end{pmatrix}\begin{pmatrix}\cos\theta_c & 0 & -\sin\theta_c\\ 0 & 1 & 0\\ \sin\theta_c & 0 & \cos\theta_c\end{pmatrix}. \tag{13}$$

The rotation matrix connecting crystal and laboratory coordinate systems adopted in this work is defined by Eq. (13). Of course, other commonly used rotation procedures exist. Rotation by two Euler angles, for example, are written not as R_{zy}, but as R_{yz}, where the azimuthal rotation is applied first. These resulting rotations are not equal and they do not have a unique correspondence using just two Euler angles. Although what description to adopt is a matter of taste, it should be clearly stated to avoid misinterpretations about any result obtained.

3. Refractive indexes

A wave-vector unitary propagation vector $\hat{\mathbf{k}}$ written in the laboratory coordinates (θ,ϕ), $\hat{\mathbf{k}}=(\sin\theta\cos\phi,\sin\theta\sin\phi,\cos\theta)$ is transformed to a vector $\hat{\mathbf{s}}$ in the crystal medium by $\hat{\mathbf{s}}=R_{zy}\cdot\hat{\mathbf{k}}$. The resulting pump, signal, and idler unitary wave vectors could then be plugged into Eq. (12) to provide the corresponding refraction indexes in a uniaxial crystal such as the BBO. One obtains

$$n=n_o, \tag{14}$$

$$n' = \frac{n'_e n'_o}{\sqrt{n_i'^2(\cos\theta_c\cos\theta' + \cos\phi'\sin\theta_c\sin\theta')^2 + n_o'^2[(\cos\theta'\sin\theta_c - \cos\theta_c\cos\phi'\sin\theta')^2 + \sin^2\theta'\sin^2\phi']}}, \quad (15)$$

$$n_P = \frac{n_{P,e}n_{P,o}}{\sqrt{n_{P,e}^2\cos^2\theta_c + n_{P,o}^2\sin^2\theta_c}}. \quad (16)$$

It is easy to observe that propagation under *eo* polarizations do not present azimuthal symmetry. However, the overall symmetry for SPDC depend on other terms as well.

4. Sellmeier equations

The refractive indexes in the principal axes, $n_{P,e}$, $n_{P,o}$, n_o, n_e, n'_o, and n'_e are usually obtained experimentally and represented by parametric equations representative of the microscopic physics involved. These equations, known as Sellmeier's equations, have a wide applicability due to its success to represent the refraction index of low absorption crystals as a real function of wavelength. They are based on the form of an oscillator response to an applied force or, as a microscopic theory for the response of bound electrons in a solid to an applied electric field (see Ref. [10], Sec. 2.3) $\mathbf{r}=e\mathbf{E}/[m(\omega_0^2-\omega^2)]$ or $P=Ner\sim\chi^{(1)}E\sim[(n^2-1)/4\pi]E$ and assumes the form $n^2=a+b/(\lambda^2-c)-d\lambda^2$. The constants a to d have to be experimentally determined for each crystal along ordinary and extraordinary propagation directions and at every desired temperature. An experimental fit to this phenomenological equation may give a very good numerical representation of the refractive indexes in a quite broad frequency range. The d term is a first corrective term of a possible series of even terms in λ. The assumption of reality for the fields **D** and **E** and their causal connection imposes the *even* dependence on λ for a real dielectric constant [11]. This way, the first terms are

$$n_o(\lambda)^2 = a - \frac{b}{\lambda^2 - c} - d\lambda^2, \quad n_e(\lambda)^2 = e - \frac{f}{\lambda^2 - g} - h\lambda^2. \quad (17)$$

Reference [12], for example, presents the experimental values $a=2.7405$, $b=0.0184$, $c=0.0179$, $d=0.0155$, $e=2.3730$, $f=0.0128$, $g=0.0156$, $h=0.0044$ to represent BBO's refractive indexes along the crystal axes (λ are given in μm in these equations).

5. Longitudinal condition

As the refractive indexes are now defined and the wave vectors $k=(2\pi/\lambda)n$ can be calculated for general angles with adequate Sellmeier parameters, Eq. (9),

$$-k_P + (k\cos\theta + k'\cos\theta') \simeq \frac{2\pi}{l_c},$$

can be solved. Due to the complexity dependence of the refractive indexes in the angles, this equation may not be solved analytically in a general case. Numerical solutions can be found and will determine the angles where the SPDC process is more efficient. For a type-II process in BBO, for example, Fig. 2 shows a plot obtained from the numerical solutions. The obtained numerical solutions can be even parametrized for simplicity. This way, polar angles giving SPDC rings are closely represented by

$$\theta_s = \arcsin(\zeta[\cos(\phi_s - \pi) + \sqrt{\cos^2(\phi_s - \pi) + \eta}] + \nu\exp\{-\nu\sin^2[(\phi_s - \pi)/2]\}\cos[2(\phi_s - \pi)]) \quad (18)$$

and

$$\theta_i = \arcsin\{\zeta(\cos\phi_i + \sqrt{\cos^2\phi_i + \eta}) + \nu\exp[-\nu\sin^2(\phi_i/2)]\cos 2\phi_i\}, \quad (19)$$

where $\zeta\simeq 0.034$, $\eta\simeq 0.797$, $\nu\simeq 0.0016$, $\mu\simeq 3.45$. These equations give the thin black lines in Fig. 2.

It has to be emphasized that these angles are described within the medium. Straightforward application of Snell's law gives the angles outside of the crystal.

B. Transverse equations

The equation $f_{\text{transv}}=\pi^2 4^{-l}|A_{lp}|^2(l_c z_R/k_P)^2 e^{-\xi}\xi^l L_p^l(\xi)^2$ together with the obtained polar angles given by Eqs. (18) and (19) define the loci of possibly entangled azimuthal angles that maximize $F_{s,s'}(\mathbf{k},\mathbf{k}')$. Finding the analytical maxima for f_{transv} is not a trivial task and will not be attempted here. However, for specific values of p and l this is usually a simple task. For example, Fig. 3 shows a plot of $f_{\text{transv}}/[\pi^2 4^{-l}|A_{lp}|^2(l_c z_R/k_P)^2]$ for $p=0$ and $l=4$. It is easy to find the maximum at $\xi_{04}\simeq 15.9491$. This defines the value $\rho_k^2(p=0,l=4)=(k_P/zR)\xi_{04}$ that maximizes the signal and idler emissions. From the transverse equation

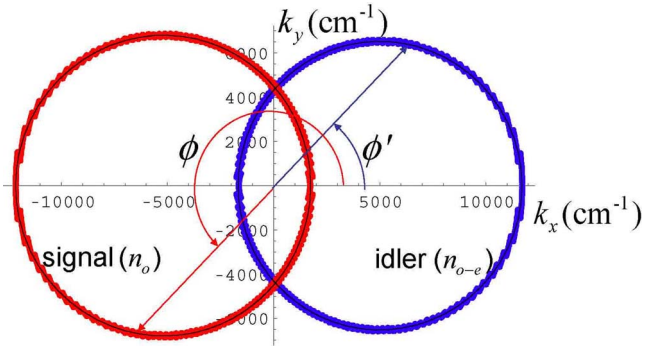

FIG. 2. (Color online) Signal and idler rings obtained from numerical solutions and thin solid lines obtained from fitting the numerical equations with Eqs. (18) and (19).

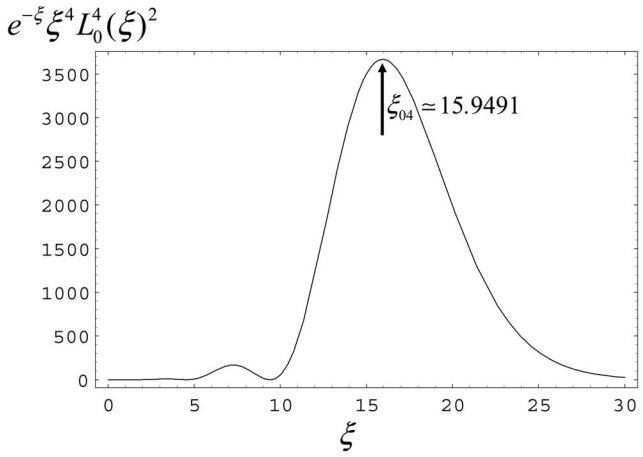

FIG. 3. (Color online) $e^{-\xi}\xi^4 L_0^4(\xi)^2$ as a function of ξ.

$$\rho_k^2 = \Delta k_x^2 + \Delta k_y^2 = \rho^2 + \rho'^2 + 2\rho\rho' \cos(\phi - \phi') \simeq \frac{k_P}{z_R}\xi_{04}, \tag{20}$$

and using the polar angle dependence given by Eqs. (18) and (19) this equation can be solved for the azimuthal angles ϕ and ϕ'. Figure 4 shows the numerical dependence found between these angles. While the condition $\phi' = \phi + \pi$ is an approximated one, some deviations exist that may be meaningful in some applications. These deviations are more apparent near azimuthal angles close to zero. The thin solid lines in Fig. 4 were obtained by fit, giving Eqs. (21),

$$\phi'_+ = 3.1836 + 0.3631e^{-0.4653\phi^2} + 0.9999\phi,$$

$$\phi'_- = 3.0996 - 0.3631e^{-0.4653\phi^2} + 0.9999\phi. \tag{21}$$

The average azimuthal angle from these two equations is

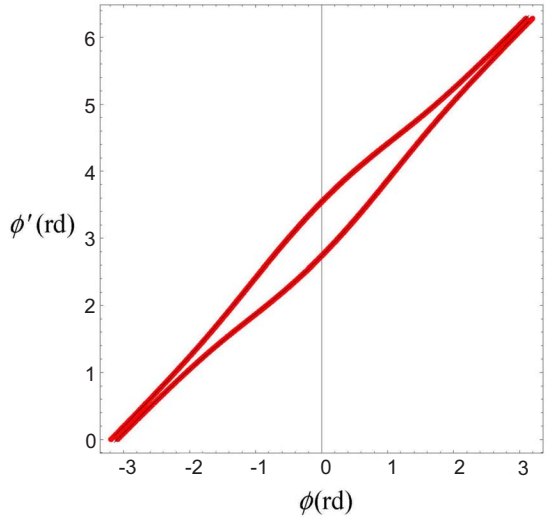

FIG. 4. (Color online) Idler azimuthal angle versus signal azimuthal angle obtained numerically from Eq. (20). The thin solid lines were obtained from Eqs. (21).

$$\phi' = \frac{\phi'_+ + \phi'_-}{2} = \phi + \pi. \tag{22}$$

Reference [2] pointed out that perfect transfer of OAM from the pump to the SPDC photons demands azimuthal symmetry for $|F_{s,s'}(\mathbf{k},\mathbf{k}')|^2$ around the pump propagation direction (quantization axis). Lack of azimuthal symmetry causes partial transfer of OAM. To illustrate this partial transfer, Fig. 5 shows transverse coincidence structures expected for degenerate noncollinear type-II SPDC in a BBO crystal (see Ref. [9] for a type-II experiment). Calculated structures represent the detection probability for signal and idler photons within small $\Delta\omega\Delta\omega'\Delta\theta\Delta\theta'\Delta\phi\Delta\phi'$ around phase matching conditions [here $\sin x/x \to 1$ and $dk \simeq (n/c)d\omega$],

$$P_{\text{scatt}} \simeq \frac{1}{|A_{\mathbf{k},s;\mathbf{k}',s'}|^2}\left|\frac{d^3k d^3k'}{d\omega d\omega' d\theta d\theta' d\phi d\phi'} F_{s,s'}(\mathbf{k},\mathbf{k}')\right|^2 \tag{23}$$

(excluding existing geometric effects given by $A_{\mathbf{k},s;\mathbf{k}',s'}$). The lack of azimuthal symmetry in type-II SPDC is reflected on the coincidence structures (even with the neglect of $|A_{\mathbf{k},s;\mathbf{k}',s'}|^2$) that show highly asymmetric coincidence donut-like pattern. Asymmetric structures should then be expected in type-II with OAM. The $A_{\mathbf{k},s;\mathbf{k}',s'}$ contribution (to be shown ahead) is non-negligible, but presents no sharp variations for the structures. Figure 6 shows some polarization vectors along the signal and idler rings.

V. NONLINEAR POLARIZABILITY

The SPDC efficiency is directly proportional to the nonlinear polarizability vector $\mathbf{P} = \Sigma_i A_{i,(\mathbf{k},s;\mathbf{k}',s')} \hat{x}_{i,cr}$ with components $A_{i,(\mathbf{k},s;\mathbf{k}',s')}$ given by the product of the tensor $\chi^{(2)}_{1jk}$ and components of the unitary polarization vectors

$$A_{i,(\mathbf{k},s;\mathbf{k}',s')} = \chi^{(2)}_{ijk}[(\mathbf{e}_{\mathbf{k},s})^*_j (\mathbf{e}_{\mathbf{k}',s'})^*_k + (\mathbf{e}_{\mathbf{k}',s'})^*_j (\mathbf{e}_{\mathbf{k},s})^*_k]. \tag{24}$$

The interaction energy V_I is given by the product of the laser field polarization and the nonlinear polarizability vector, $V_I = \mathbf{E}_P \cdot \mathbf{P}$. Up to now, all equations have been developed using laboratory coordinates. In order to keep the same reference system, all quantities in $A_{\mathbf{k},s;\mathbf{k}',s'}$ have to be referred to the laboratory coordinate system. Usually, the nonlinear dielectric tensor is given in the crystal axes and a coordinate transformation to the laboratory axes is necessary. $A_{\mathbf{k},s;\mathbf{k}',s'}$ involves the nonlinear tensor $\chi^{(2)}$ and the unitary polarization vectors $\mathbf{e}_{\mathbf{k},s}$. These constitutive elements will be considered in the following sections. The nonlinear tensor can be written in the laboratory coordinate system and multiplied by the components of the unitary polarization vector in the same reference system or, alternately, $\chi^{(2)}_{ijk}$ and the unitary polarization vectors can be written in the crystal reference system and the resulting vector component rotated to the laboratory coordinate system. This last method will be followed.

The susceptibility tensor $\chi^{(2)}_{qmn}$ for the class of uniaxial crystals can be written in a contracted form as $\chi^{(2)}_{qmn} \to \chi^{(2)}_{ql} \equiv 2d_{ql}$ as indicated in Table I. This way,

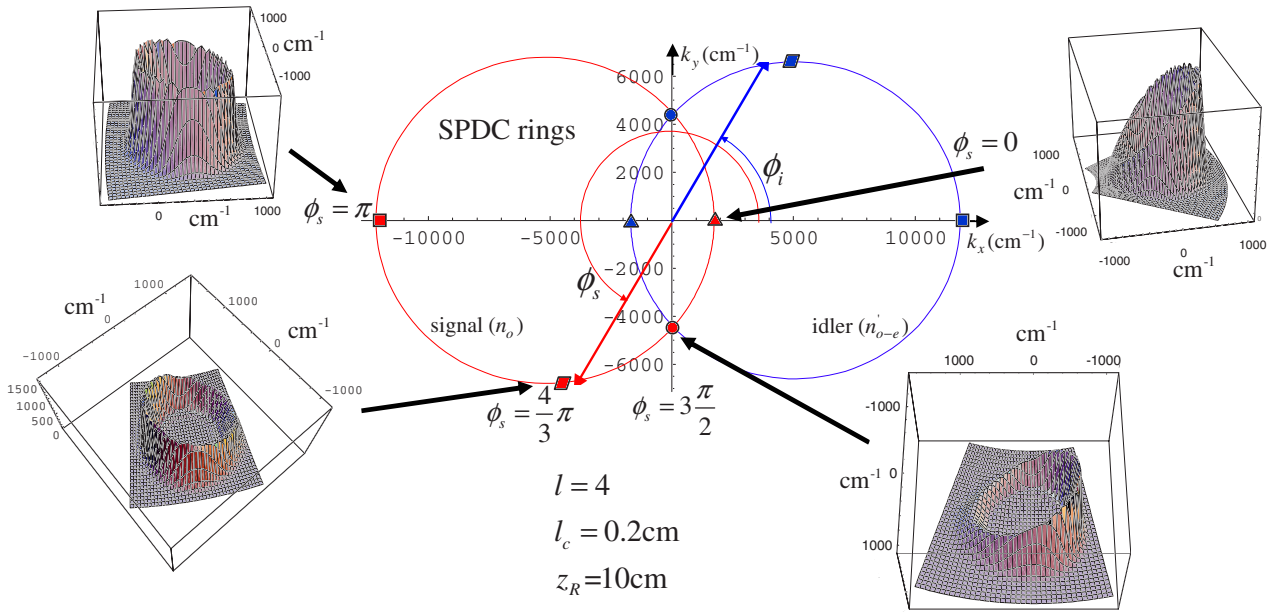

FIG. 5. (Color online) Calculated transverse coincidence-count structures on s ring with point detector on i ring. All angles are laboratory angles, but inside the crystal. The crystal is tilted with the laser beam at $\theta_c = 49.7°$ ($\phi_c = 0$) from the crystal c axis. The laser wavelength is $\lambda_P = 3511$ Å ($\hat{\mathbf{e}}_1 = \hat{\mathbf{x}}$) and the principal refractive indexes are $n_{P,o} = 1.707$, $n_{P,e} = 1.578$, $n_o = n'_o = 1.665$, $n'_e = 1.548$.

$$\chi^{(2)} = 2\begin{pmatrix} d_{11} & d_{12} & d_{13} & d_{14} & d_{15} & d_{16} \\ d_{21} & d_{22} & d_{23} & d_{24} & d_{25} & d_{26} \\ d_{31} & d_{32} & d_{33} & d_{34} & d_{35} & d_{36} \end{pmatrix}. \tag{25}$$

To calculate the unitary polarization vectors, one may write the electric displacement $\mathbf{D}$ in the crystal principal axis, where $\epsilon_{ij} = \epsilon_{ii}\delta_{ij}$ results $D_i = \epsilon_{ii}\delta_{ii}E_j = n^2(E_i - s_i s_k E_k)$ or

$$[n_x^2 - n^2(1 - s_x^2)]E_x + n^2 s_x s_y E_y + n^2 s_x s_z E_z = 0,$$

$$n^2 s_x s_y E_x + [n_y^2 - n^2(1 - s_y^2)]E_y + n^2 s_y s_z E_z = 0,$$

$$n^2 s_x s_z E_x + n^2 s_y s_z E_y + [n_z^2 - n^2(1 - s_z^2)]E_z = 0. \tag{26}$$

This set of equations give the possible electric field amplitudes for specific propagation directions and refractive indexes n. Without developing general solutions, one may look for a solution for the signal photons propagating with *ordinary* refraction index n_o. Writing $n_x = n_y = n_o$ and $n_z = n_e$ for the idler's refractive indexes, the electric field components in the medium are obtained and normalized resulting in

$$\hat{\mathbf{e}}_{o,cr} = (-\sin\theta_{cr}, \cos\theta_{cr}, 0). \tag{27}$$

To calculate the unitary polarization vector for *extraordinary propagation*, one may observe that in the crystal medium the Poynting vector form a set of orthogonal axes with the electric field and the magnetic field. At the same time, the electric displacement may not be along with the electric field, but is normal to the propagation vector in the medium. Equation (26) can be particularized for this case as well. However, for simplicity, one may look for field solutions that give a unitary polarization vector for the extraordinary propagation $\hat{\mathbf{e}}'_{cr}$ orthogonal both to $\hat{\mathbf{e}}_{cr}$ and to its unitary propagation vector $\hat{\mathbf{s}}' = s'_x\hat{\mathbf{x}} + s'_y\hat{\mathbf{y}} + s'_z\hat{\mathbf{z}}$. This gives

$$\hat{\mathbf{e}}'_{e,cr} = (-\cos\theta'_{cr}\cos\phi'_{cr}, -\cos\theta'_{cr}\sin\phi'_{cr}, \sin\theta'_{cr}\cos\phi'_{cr}). \tag{28}$$

See Fig. 6 for an example of unitary polarization vectors in. BBO type II

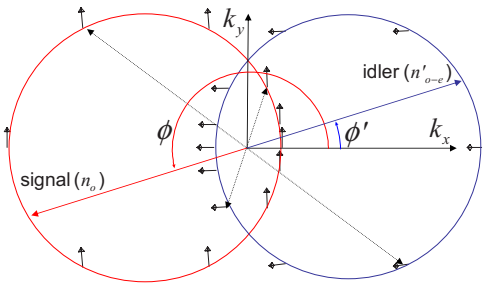

FIG. 6. (Color online) Polarization vectors (pairs) along the signal and idler rings in SPDC type II.

A. Nonlinear polarizabilities in the crystal reference system

Calculation of the nonlinear polarizability components $A_{i,(\mathbf{k},s;\mathbf{k}',s')}$ demands specification of $[(\mathbf{e}_{\mathbf{k},s})^*_j(\mathbf{e}_{\mathbf{k}',s'})^*_k + (\mathbf{e}_{\mathbf{k}',s'})^*_j(\mathbf{e}_{\mathbf{k},s})^*_k]$ for all SPDC possible cases. The question

TABLE I. Contractions for tensor indexes.

Indexes	Contractions					
mn	11	22	33	23,32	31,13	12,21
l	1	2	3	4	5	6

mark in Eq. (29) represents the need for these choices. The possible cases (o,o), (e,e), (o,e), and (o,e) are detailed in the Appendix,

$$\mathbf{P}=\begin{pmatrix} A_{1,(\mathbf{k},s;\mathbf{k}',s')} \\ A_{2,(\mathbf{k},s;\mathbf{k}',s')} \\ A_{3,(\mathbf{k},s;\mathbf{k}',s')} \end{pmatrix} = 4\begin{pmatrix} d_{11} & d_{12} & d_{13} & d_{14} & d_{15} & d_{16} \\ d_{21} & d_{22} & d_{23} & d_{24} & d_{25} & d_{26} \\ d_{31} & d_{32} & d_{33} & d_{34} & d_{35} & d_{36} \end{pmatrix} \times \begin{pmatrix} e_1e_1' \\ e_2e_2' \\ e_3e_3' \\ e_2e_3'+e_3e_2' \\ e_1e_3'+e_3e_1' \\ e_1e_2'+e_2e_1' \end{pmatrix}. \quad (29)$$

Using the appropriate polarization cases the signal and idler nonlinear polarizability $\mathbf{P}_{oo}$, $\mathbf{P}_{ee}$, $\mathbf{P}_{eo}$, and $\mathbf{P}_{oe}$ are calculated (see Appendix). These nonlinear polarizabilities cover all possibilities of light excitation in uniaxial crystals.

B. Nonlinear polarizabilities in the laboratory reference system

For SPDC it is usual to have the crystal rotated by convenient angles referred to the laboratory reference system x,y,x,θ,ϕ instead of $x_{cr},y_{cr},x_{cr},\theta_{cr},\phi_{cr}$. A laser with amplitude E_P polarized along direction $\hat{\mathbf{e}}$ will define the light matter interaction to be analyzed. In this work it is chosen to have the nonlinear polarizability $\mathbf{P}$ rotated to the laboratory reference system; this transforms $\mathbf{P}\rightarrow\mathbf{P}_{\text{lab}}$.

Equations (A5), (A6), (A8), and (A10) can be written in the laboratory coordinate system under rotation given by R_{zy}^{-1}; $\mathbf{P}_{\alpha\beta;\text{lab}}=R_{zy}^{-1}\cdot\mathbf{P}_{\alpha\beta}$ $(\alpha\beta=oo,ee,eo,oe)$. For an example, one can choose a laser amplitude $\mathbf{E}_P=E_P\hat{\mathbf{x}}$ and obtain for o,e polarizability

$$\begin{aligned} V_{I,oe} &= -E_P\hat{\mathbf{x}}\cdot(R_{zy}^{-1}\cdot\mathbf{P}_{oe}) = \cos\theta_c\cos\phi_c[-d_{14}\cos\phi_{cr}\sin\theta_{cr}'+d_{12}\cos\theta_{cr}'\cos\phi_{cr}\sin\phi_{cr}'-d_{11}\cos\theta_{cr}'\cos\phi_{cr}'\sin\phi_{cr} \\ &+d_{15}\sin\theta_{cr}'\sin\phi_{cr}+d_{16}(\cos\theta_{cr}'\cos\phi_{cr}'\cos\phi_{cr}-\cos\theta_{cr}'\sin\phi_{cr}'\sin\phi_{cr})]-\cos\theta_c\sin\phi_c[-d_{24}\cos\phi_{cr}\sin\theta_{cr}' \\ &+d_{22}\cos\theta_{cr}'\cos\phi_{cr}\sin\phi_{cr}'-d_{21}\cos\theta_{cr}'\cos\phi_{cr}'\sin\phi_{cr}+d_{25}\sin\theta_{cr}'\sin\phi_{cr}+d_{26}(\cos\theta_{cr}'\cos\phi_{cr}'\cos\phi_{cr} \\ &-\cos\theta_{cr}'\sin\phi_{cr}'\sin\phi_{cr})]+\sin\theta_c[-(d_{34}\cos\phi_{cr}\sin\theta_{cr}')+d_{32}\cos\theta_{cr}'\cos\phi_{cr}\sin\phi_{cr}'-d_{31}\cos\theta_{cr}'\cos\phi_{cr}'\sin\phi_{cr} \\ &+d_{35}\sin\theta_{cr}'\sin\phi_{cr}+d_{36}(\cos\theta_{cr}'\cos\phi_{cr}'\cos\phi_{cr}-\cos\theta_{cr}'\sin\phi_{cr}'\sin\phi_{cr})]. \end{aligned} \quad (30)$$

For a crystal where the dominant coefficients are d_{11}, d_{22}, and d_{15} (e.g., BBO), $V_{I,oe}$ simplifies to

$$\begin{aligned} V_{I,oe} &= -(d_{22}\cos\theta_c\cos\theta_{cr}'\cos\phi_{cr}\sin\phi_c\sin\phi_{cr}') \\ &+\cos\theta_c\cos\phi_c(-d_{11}\cos\theta_{cr}'\cos\phi_{cr}'\sin\phi_{cr} \\ &+d_{15}\sin\theta_{cr}'\sin\phi_{cr}). \end{aligned} \quad (31)$$

Replacing $\theta_{cr}'\rightleftharpoons\theta_{cr}\phi_{cr}'\rightleftharpoons\phi_{cr}$ in Eq. (31) gives $V_{I,eo}$ for BBO.

Crystal to laboratory reference system. If one wishes to have $V_{I,oe}$ (or any other interaction energy term) written under laboratory angles (θ,ϕ), the connection between angles in these two systems have to be found. Given a unitary vector $\mathbf{v}=(\sin\theta\cos\phi,\sin\theta\sin\phi,\cos\theta)$ in the laboratory reference system, the rotation R_{zy} brings it to the crystal coordinate system (or the inverse rotation to move the reference system). Assuming that vector components in the crystal reference system can be written as $\mathbf{v}=\mathbf{v}_{cr}=(\sin\theta_{cr}\cos\phi_{cr},\sin\theta_{cr}\sin\phi_{cr},\cos\theta_{cr})$, a connection between the medium and the laboratory angles can be found. This way

$$\theta_{cr}=\arccos(\cos\theta_c\cos\theta+\cos\phi\sin\theta_c\sin\theta), \quad (32)$$

$$\phi_{cr}=\arccos\left[\frac{\sqrt{n1+n2+n3}}{\sqrt{(-1+\cos\theta_c\cos\theta+\cos\phi\sin\theta_c\sin\theta)(1+\cos\theta_c\cos\theta+\cos\phi\sin\theta_c\sin\theta)}}\right], \quad (33)$$

where

$$\begin{aligned} n1 &= -1+\cos\phi^2\sin\theta_c^2\sin\theta^2+\cos\theta_c^2(\cos\theta^2 \\ &+\cos\phi^2\sin\theta^2\sin\phi_c^2), \end{aligned} \quad (34)$$

$$n2=(\cos\theta\sin\theta_c\sin\phi_c+\cos\phi_c\sin\theta\sin\phi)^2, \quad (35)$$

$$\begin{aligned} n3 &= 2\cos\theta_c\cos\phi_c\cos\phi\sin\theta(\cos\theta\cos\phi_c\sin\theta_c \\ &-\sin\theta\sin\phi_c\sin\phi). \end{aligned} \quad (36)$$

Replacing in $V_{I,oe}$ the appropriate angle given by the θ_{cr} or ϕ_{cr} above, $V_{I,oe}$ is determined in terms of the laboratory angles. The procedure is straightforward but the resulting expression is quite long.

C. A method for determination of nonlinear coefficients

Knowing the precise rotation angles between the crystal reference system, the laboratory system, and phase matching angles, it was shown that all elements to determine the signal and idler scattering probabilities [wave state amplitude, Eq. (7)] can be obtained in detail. From these information, transverse coincidence structures can be calculated (see Ref. [9]) and by integration over the angle variables for signal (or idler) the angular dependence of the idler (or signal) intensity can be obtained. Aside from obtaining a detailed picture of SPDC process, it should be pointed out that use of these equations allows one to obtain directly through simple intensity measurements [14] the nonlinear coefficients d_{ij}. This can be done by fit of the existing experimental angle dependence to the theoretical elements presented, including numerical integrations indicated. Although this analysis is not the object of this work, it is interesting to observe that considering just an integration over the nonlinear polarizability, neglecting the contribution from $\tilde{\psi}_{lp}(\Delta\mathbf{k})$, leads to azimuthal asymmetries. For example, on the transverse plane (x,y), normal to the pump laser,

$$\begin{aligned} P_{oe,x,y} = \{&\cos\theta_c[d_{15}\cos\phi_c\sin\theta'_{cr}\sin\phi_{cr} \\ &- \cos\theta'_{cr}(d_{22}\cos\phi_{cr}\sin\phi_c\sin\phi'_{cr} \\ &+ d_{11}\cos\phi_c\cos\phi'_{cr}\sin\phi_{cr})], \\ &\times d_{22}\cos\theta'_{cr}\cos\phi_c\cos\phi_{cr}\sin\phi'_{cr} \\ &+ [-(d_{11}\cos\theta'_{cr}\cos\phi'_{cr}) + d_{15}\sin\theta'_{cr}] \\ &\times\sin\phi_c\sin\phi_{cr},0\}, \end{aligned} \tag{37}$$

$$\left(\int_0^{2\pi} P_{oe,x,y}d\phi'_{cr}\right)^2 = 4d_{15}^2\pi^2\sin^2\theta'_{cr}\sin^2\phi_{cr}(\cos^2\theta_c\cos^2\phi_c + \sin^2\phi_c). \tag{38}$$

The (simplified) azimuthal dependence indicated by Eq. (38) shows a variable intensity for the SPDC rings (see experimental result in Ref. [14]).

D. Modulation by external fields

Extending our knowledge about the microscopic behavior of the light-matter interactions in SPDC would help us to examine other possibilities to use entangled photon pairs. External generalized fields can be added to allow modulations to be applied to these systems. Pressure, electric and magnetic fields are natural candidates to exert different modifications on the optically nonlinear medium. The virtual character of the SPDC process do not allow direct access to energy levels involved ($\Delta t\to 0$ leads to $\Delta E\to\infty$) but, nevertheless, it does not exclude one to observe important effects related to these virtual processes. For example, a magnetic field may modify electronic levels with detectable effects on SPDC (type I or type II). Induced defects can also be used to probe for local symmetry variations in crystals [8]. Several tools can be used to explore this fundamental problem of OAM transfer by a nonlinear medium and may lead to a better understanding of the underlying microscopic physics. Future quantum applications of OAM entanglement, such as quantum computation or teleportation, may depend on a deep understanding of these OAM transfer process to achieve a very efficient use and control of quantum entanglements.

VI. CONCLUSIONS

Explicit calculation of the equations determining SPDC processes when OAM is involved were provided for crystals of uniaxial symmetry. The light-matter nonlinear polarizability components $A_{i,(\mathbf{k},s;\mathbf{k}',s')}$ were calculated giving the complete angular dependence in the crystal reference system as well as in the laboratory system. The Fourier transform $\tilde{\psi}_{lp}(\Delta\mathbf{k})$ was analytically calculated and approximations used were discussed. Phase matching conditions were obtained and it was shown that spatial transverse coincidence structures can be calculated. In Ref. [2] it was shown that whenever $|F(\mathbf{k}_s,\mathbf{k}_i)|^2$ [see Eq. (2)] lacks azimuthal symmetry, an expansion of $F(\mathbf{k}_s,\mathbf{k}_i)$ in terms of the azimuthal angles reveals that—despite the energy conservation condition—the initial orbital angular momentum l connected with a photon in the incoming mode may not be transmitted to the SPDC pair. Either the energy and momentum goes back as a pump photon or the momentum transfer may be partial (phase correlation loss), with the signal and idler carrying the OAM value $l'\neq l$. The obtained equations for $A_{i,(\mathbf{k},s;\mathbf{k}',s')}$ and $\tilde{\psi}_{lp}(\Delta\mathbf{k})$ allows one to make these expansions to study specific cases. It is expected that the explicit treatment of the probability amplitude given in this work may allow further developments in the study of quantum images in SPDC process involving OAM. Analytical tools are then provided to indicate whether a specific SPDC process may or may not transfer OAM to the conjugate photons. Straightforward extensions of this work can also be done such as to obtain output profiles in second harmonic generation where one or both of the input beams are in OAM states. The symmetry properties of the light-matter interaction will be revealed by the up-converted beam.

ACKNOWLEDGMENT

This work was supported by the U. S. Army Research Office Multidisciplinary University Research Initiative Grant No. W911NF-05-1-0197 on Quantum Imaging.

APPENDIX

Expansion of the vector products give the cases (o,o), (e,e), (o,e) and (o,e):

$$\begin{pmatrix} e_1e'_1 \\ e_2e'_2 \\ e_3e'_3 \\ e_2e'_3+e_3e'_2 \\ e_1e'_3+e_3e'_1 \\ e_1e'_2+e_2e'_1 \end{pmatrix}_{o,o} = \begin{pmatrix} e_{o,1}e'_{o,1} \\ e_{o,2}e'_{o,2} \\ e_{o,3}e'_{o,3} \\ e_{o,2}e'_{o,3}+e_{o,3}e'_{o,2} \\ e_{o,1}e'_{o,3}+e_{o,3}e'_{o,1} \\ e_{o,1}e'_{o,2}+e_{o,2}e'_{o,1} \end{pmatrix} = \begin{pmatrix} \sin\phi_{cr}\sin\phi'_{cr} \\ \cos\phi_{cr}\cos\phi'_{cr} \\ 0 \\ 0 \\ 0 \\ -\cos\phi_{cr}\sin\phi'_{cr}-\sin\phi_{cr}\cos\phi'_{cr} \end{pmatrix}, \tag{A1}$$

$$\begin{pmatrix} e_1e'_1 \\ e_2e'_2 \\ e_3e'_3 \\ e_2e'_3+e_3e'_2 \\ e_1e'_3+e_3e'_1 \\ e_1e'_2+e_2e'_1 \end{pmatrix}_{e,e} = \begin{pmatrix} e_{e,1}e'_{e,1} \\ e_{e,2}e'_{e,2} \\ e_{e,3}e'_{e,3} \\ e_{e,2}e'_{e,3}+e_{e,3}e'_{e,2} \\ e_{e,1}e'_{e,3}+e_{e,3}e'_{e,1} \\ e_{e,1}e'_{e,2}+e_{e,2}e'_{e,1} \end{pmatrix} = \begin{pmatrix} \cos\theta_{cr}\cos\theta'_{cr}\cos\phi_{cr}\cos\phi'_{cr} \\ \cos\theta_{cr}\cos\theta'_{cr}\sin\phi_{cr}\sin\phi'_{cr} \\ \sin\theta_{cr}\sin\theta'_{cr} \\ -\sin\theta_{cr}\cos\theta'_{cr}\sin\phi'_{cr}-\cos\theta_{cr}\sin\phi_{cr}\sin\phi'_{cr} \\ -\cos\theta_{cr}\cos\phi_{cr}\sin\theta'_{cr}-\sin\theta_{cr}\cos\theta'_{cr}\cos\phi'_{cr} \\ \cos\theta_{cr}\cos\theta'_{cr}(\cos\phi_{cr}\sin\phi'_{cr}+\sin\phi_{cr}\cos\phi'_{cr}) \end{pmatrix}, \tag{A2}$$

$$\begin{pmatrix} e_1e'_1 \\ e_2e'_2 \\ e_3e'_3 \\ e_2e'_3+e_3e'_2 \\ e_1e'_3+e_3e'_1 \\ e_1e'_2+e_2e'_1 \end{pmatrix}_{e,o} = \begin{pmatrix} e_{e,1}e'_{o,1} \\ e_{e,2}e'_{o,2} \\ e_{e,3}e'_{o,3} \\ e_{e,2}e'_{o,3}+e_{e,3}e'_{o,2} \\ e_{e,1}e'_{o,3}+e_{e,3}e'_{o,1} \\ e_{e,1}e'_{o,2}+e_{e,2}e'_{o,1} \end{pmatrix} = \begin{pmatrix} -\cos\theta_{cr}\cos\phi_{cr}\sin\phi'_{cr} \\ \cos\theta_{cr}\sin\phi_{cr}\cos\phi'_{cr} \\ 0 \\ -\sin\theta_{cr}\cos\phi'_{cr} \\ \sin\theta_{cr}\sin\phi'_{cr} \\ \cos\theta_{cr}\cos\phi_{cr}\cos\phi'_{cr}-\cos\theta_{cr}\sin\phi_{cr}\sin\phi'_{cr} \end{pmatrix}, \tag{A3}$$

$$\begin{pmatrix} e_1e'_1 \\ e_2e'_2 \\ e_3e'_3 \\ e_2e'_3+e_3e'_2 \\ e_1e'_3+e_3e'_1 \\ e_1e'_2+e_2e'_1 \end{pmatrix}_{o,e} = \begin{pmatrix} e_{o,1}e'_{e,1} \\ e_{o,2}e'_{e,2} \\ e_{o,3}e'_{e,3} \\ e_{o,2}e'_{e,3}+e_{o,3}e'_{e,2} \\ e_{o,1}e'_{e,3}+e_{o,3}e'_{e,1} \\ e_{o,1}e'_{e,2}+e_{o,2}e'_{e,1} \end{pmatrix} = \begin{pmatrix} -\sin\phi_{cr}\cos\theta'_{cr}\cos\phi'_{cr} \\ \cos\phi_{cr}\cos\theta'_{cr}\sin\phi'_{cr} \\ 0 \\ -\cos\phi_{cr}\sin\theta'_{cr} \\ \sin\phi_{cr}\sin\theta'_{cr} \\ \cos\phi_{cr}\cos\theta'_{cr}\cos\phi'_{cr}-\sin\phi_{cr}\cos\theta'_{cr}\sin\phi'_{cr} \end{pmatrix}. \tag{A4}$$

For the collinear and degenerate propagation, these vectors give the particular cases described in Ref. [13].

The nonlinear polarizabilities are obtained in a straightforward way, giving

$$\begin{aligned} \mathbf{P}_{oo} = [&\sin\phi'_{cr}(d_{11}\sin\phi_{cr}-d_{16}\cos\phi_{cr}) \\ &+\cos\phi'_{cr}(d_{12}\cos\phi_{cr}-d_{16}\sin\phi_{cr}), \\ &\sin\phi'_{cr}(d_{21}\sin\phi_{cr}-d_{26}\cos\phi_{cr}) \\ &+\cos\phi'_{cr}(d_{22}\cos\phi_{cr}-d_{26}\sin\phi_{cr}), \\ &\sin\phi'_{cr}(d_{31}\sin\phi_{cr}-d_{36}\cos\phi_{cr}) \\ &+\cos\phi'_{cr}(d_{32}\cos\phi_{cr}-d_{36}\sin\phi_{cr})], \end{aligned} \tag{A5}$$

$$\mathbf{P}_{ee} = [P_{ee,xcr}, P_{ee,ycr}, P_{ee,zcr}], \tag{A6}$$

where

$$\begin{aligned} P_{ee,xcr} = &\sin\theta'_{cr}[d_{13}\sin\theta_{cr}-\cos\theta_{cr}(d_{15}\cos\phi_{cr}+d_{14}\sin\phi_{cr})] \\ &+\cos\theta'_{cr}[-\sin\theta_{cr}(d_{15}\cos\phi'_{cr}+d_{14}\sin\phi'_{cr}) \\ &+\cos\theta_{cr}(d_{11}\cos\phi'_{cr}\cos\phi_{cr}+d_{16}\cos\phi_{cr}\sin\phi'_{cr} \\ &+d_{16}\cos\phi'_{cr}\sin\phi_{cr}+d_{12}\sin\phi'_{cr}\sin\phi_{cr})], \\ P_{ee,ycr} = &\sin\theta'_{cr}[d_{23}\sin\theta_{cr}-\cos\theta_{cr}(d_{25}\cos\phi_{cr}+d_{24}\sin\phi_{cr})] \\ &+\cos\theta'_{cr}[-\sin\theta_{cr}(d_{25}\cos\phi'_{cr}+d_{24}\sin\phi'_{cr}) \\ &+\cos\theta_{cr}(d_{21}\cos\phi'_{cr}\cos\phi_{cr}+d_{26}\cos\phi_{cr}\sin\phi'_{cr} \\ &+d_{26}\cos\phi'_{cr}\sin\phi_{cr}+d_{22}\sin\phi'_{cr}\sin\phi_{cr})], \\ P_{ee,zcr} = &\sin\theta'_{cr}[d_{33}\sin\theta_{cr}-\cos\theta_{cr}(d_{35}\cos\phi_{cr}+d_{34}\sin\phi_{cr})] \\ &+\cos\theta'_{cr}[-\sin\theta_{cr}(d_{35}\cos\phi'_{cr}+d_{34}\sin\phi'_{cr}) \\ &+\cos\theta_{cr}(d_{31}\cos\phi'_{cr}\cos\phi_{cr}+d_{36}\cos\phi_{cr}\sin\phi'_{cr} \\ &+d_{36}\cos\phi'_{cr}\sin\phi_{cr}+d_{32}\sin\phi'_{cr}\sin\phi_{cr})]. \end{aligned} \tag{A7}$$

$$\mathbf{P}_{eo} = [P_{eo,xcr}, P_{eo,ycr}, P_{eo,zcr}], \tag{A8}$$

where

$$\begin{aligned} P_{eo,xcr} &= \sin\theta_{cr}(-d_{14}\cos\phi'_{cr} + d_{15}\sin\phi'_{cr}) \\ &+ \cos\theta_{cr}[\cos\phi'_{cr}(d_{16}\cos\phi_{cr} + d_{12}\sin\phi_{cr}) \\ &- \sin\phi'_{cr}(d_{11}\cos\phi_{cr} + d_{16}\sin\phi_{cr})], \end{aligned}$$

$$\begin{aligned} P_{eo,ycr} &= \sin\theta_{cr}(-d_{24}\cos\phi'_{cr} + d_{25}\sin\phi'_{cr}) \\ &+ \cos\theta_{cr}[\cos\phi'_{cr}(d_{26}\cos\phi_{cr} + d_{22}\sin\phi_{cr}) \\ &- \sin\phi'_{cr}(d_{21}\cos\phi_{cr} + d_{26}\sin\phi_{cr})], \end{aligned}$$

$$\begin{aligned} P_{eo,zcr} &= \sin\theta_{cr}(-d_{34}\cos\phi'_{cr} + d_{35}\sin\phi'_{cr}) \\ &+ \cos\theta_{cr}[\cos\phi'_{cr}(d_{36}\cos\phi_{cr} + d_{32}\sin\phi_{cr}) \\ &- \sin\phi'_{cr}(d_{31}\cos\phi_{cr} + d_{36}\sin\phi_{cr})]. \end{aligned} \tag{A9}$$

$$\mathbf{P}_{oe} = [P_{oe,xcr}, P_{oe,ycr}, P_{oe,zcr}], \tag{A10}$$

where

$$\begin{aligned} P_{oe,xcr} &= \sin\theta'_{cr}(-d_{14}\cos\phi_{cr} + d_{15}\sin\phi_{cr}) \\ &+ \cos\theta'_{cr}[\cos\phi_{cr}(d_{16}\cos\phi'_{cr} + d_{12}\sin\phi'_{cr}) \\ &- (d_{11}\cos\phi'_{cr} + d_{16}\sin\phi'_{cr})\sin\phi_{cr}], \end{aligned}$$

$$\begin{aligned} P_{oe,ycr} &= \sin\theta'_{cr}(-d_{24}\cos\phi_{cr} + d_{25}\sin\phi_{cr}) \\ &+ \cos\theta'_{cr}[\cos\phi_{cr}(d_{26}\cos\phi'_{cr} + d_{22}\sin\phi'_{cr}) \\ &- (d_{21}\cos\phi'_{cr} + d_{26}\sin\phi'_{cr})\sin\phi_{cr}], \end{aligned}$$

$$\begin{aligned} P_{oe,zcr} &= \sin\theta'_{cr}(-d_{34}\cos\phi_{cr} + d_{35}\sin\phi_{cr}) \\ &+ \cos\theta'_{cr}[\cos\phi_{cr}(d_{36}\cos\phi'_{cr} + d_{32}\sin\phi'_{cr}) \\ &- (d_{31}\cos\phi'_{cr} + d_{36}\sin\phi'_{cr})\sin\phi_{cr}]. \end{aligned} \tag{A11}$$

[1] A. Mair, A. Vaziri, G. Weihs, and A. Zeilinger, Nature (London) **412**, 313 (2001).

[2] H. H. Arnaut and G. A. Barbosa, Phys. Rev. Lett. **85**, 286 (2000).

[3] S. Feng, C.-H. Chen, G. A. Barbosa, and P. Kumar, e-print arXiv:quant-ph/0703187v1.

[4] S. P. Walborn, A. N. de Oliveira, R. S. Thebaldi, and C. H. Monken, Phys. Rev. A **69**, 023811 (2004).

[5] L. Mandel and E. Wolf, *Optical Coherence and Quantum Optics* (Cambridge University Press, New York, 1995). Some historical references are D. L. Weinberg, Appl. Phys. Lett. **14**, 32 (1969); D. C. Burham and D. L. Weinberg, Phys. Rev. Lett. **25**, 84 (1970); Y. B. Zel'dovich, and D. N. Klyshko, Zh. Eksp. Teor. Fiz. Pis'ma Red. **9**, 69 (1969) [JETP Lett. **9**, 40 (1969)]; W. H. Louisell, A. Yariv, and A. E. Siegman, Phys. Rev. **124**, 1646 (1961).

[6] S. Franke-Arnold, S. M. Barnett, E. Yao, J. Leach, J. Courtial, and M. Padgett, New J. Phys. **6**, 103 (2004); D. T. Pegg, S. M. Barnett, R. Zambrini, S. Franke-Arnold, and M. Padgett, *ibid.* **7**, 82 (2005).

[7] A simple azimuthal rotation of the Hamiltonian under the constraint $[J_z, H]=0$ shows azimuthal independence: $H(\Delta\phi) = \exp(i\Delta\phi J_z) H \exp(-i\Delta\phi J_z) = H + i\Delta\phi[J_z, H] + \cdots = H$.

[8] W. Hong, L. E. Halliburton, K. T. Stevens, D. Perlov, G. C. Catella, R. K. Route, and R. S. Feigelson, J. Appl. Phys. **94**, 2510 (2003).

[9] S. Feng, C.-H. Chen, G. A. Barbosa, and P. Kumar (unpublished).

[10] M. Born and E. Wolf, *Principles of Optics* (Pergamon Press, New York, 1959) p. 535.

[11] J. D. Jackson, *Classical Electrodynamics*, 3rd ed. (Wiley, New York, 1999), Sec 7.10.

[12] D. Eierl, L. Davis, S. Welsko, E. K. Graham, and A. Zalkin, J. Appl. Phys. **62**, 1968 (1987).

[13] J. E. Midwinter and J. Warner, Br. J. Appl. Phys. **16**, 1135 (1965).

[14] O. Jedrkiewicz, E. Bambrilla, M. Bache, A. Gatti, L. A. Lugiato, and P. Di Trapani, J. Mod. Opt. **53**, 575 (2006).